Agricultural and Forest Meteorology 198–199 (2014) 1–6

Contents lists available at ScienceDirect

Agricultural and Forest Meteorology

journal homepage: www.elsevier.com/locate/agrformet

Data filtering for inverse dispersion emission calculations

Thomas K. Flesch[a,*], Sean M. McGinn[b], Deli Chen[c], John D. Wilson[a], Raymond L. Desjardins[d]

[a] Department of Earth and Atmospheric Sciences, 1-22 Earth Sciences Bldg, University of Alberta, Edmonton, AB, Canada T6G 2E3
[b] Agriculture and Agri-Food Canada, 5403—1 Avenue South, Lethbridge, AB, Canada T1J 4B1
[c] Melbourne School of Land and Environment, The University of Melbourne, Melbourne 3010, VIC, Australia
[d] Agriculture and Agri-Food Canada, 960 Carling Ave., Ottawa, ON, Canada K1A 0C6

ARTICLE INFO

Article history:
Received 16 January 2014
Received in revised form 18 July 2014
Accepted 20 July 2014
Available online 11 August 2014

Keywords:
Inverse dispersion
Monin–Obukhov similarity theory
Emission measurement
Open-path laser

ABSTRACT

Inverse dispersion techniques are used to infer the emission rate of gas sources from concentration measurements and dispersion model calculations. Criteria for the selection of measurement intervals having wind conditions conducive to technique accuracy are examined on the basis of a short range tracer experiment. By introducing a supplementary condition that the measured vertical temperature gradient be quantitatively compatible with Monin–Obukhov similarity theory, it was possible to use a less stringent threshold for the friction velocity than has previous been used ($u_* \geq 0.05\,m\,s^{-1}$ instead of $\geq 0.15\,m\,s^{-1}$). Under the new criteria a larger proportion of measurement intervals are retained (76% versus 49%), while the ratio of inferred to actual emission rate Q_{LS}/Q exhibits negligible bias (average $Q_{LS}/Q = 1.00$) and an acceptably small level of random error (interval-to-interval standard deviation $\sigma_{Q/Q} = 0.25$).

1. Introduction

"Inverse dispersion" refers to the practice of inferring the atmospheric emission rate (Q) of localized gas sources from the excess concentration (C) they cause, by modelling the C–Q relationship under the existing meteorological state. The technique has proven particularly successful for calculating emissions from discrete ground level sources using nearby concentration measurements (e.g., Ferrara et al., 2014). This micrometeorological scale problem requires only an upwind and downwind gas concentration, with substantial freedom to choose convenient measurement locations. The technique does have the disadvantage that, in its most practical form, it entails idealizations that may compromise accuracy in some circumstances. Chief among these is the assumption that a dispersion model predicated on horizontally-homogeneous winds will suffice for the inversion, obviating what is (otherwise) a burdensome computation. While strictly unobstructed wind fields are the exception, fortunately a number of studies in disturbed winds have indicated that the technique can be quite robust (e.g., Wilson et al., 2010).

Different types of dispersion models can be used for inverse calculations. A common implementation combines a Lagrangian stochastic (LS) model with a Monin–Obukhov (MO) similarity theory description of the wind (Wilson et al., 2012), and to that end specialized "MO–LS" software has evolved[1]. In an agricultural context MO–LS has been used to calculate emissions from barns (Harper et al., 2010), fields (Sanz et al., 2010), cattle feedlots (Todd et al., 2011), waste storage ponds (Flesch et al., 2013), grazing cattle (McGinn et al., 2011), and many other variations of source and environment.

An MO–LS emission calculation presumes MO accurately describes the vertical profiles of the average wind and turbulent statistics. The theory posits that these properties are characterized by the friction velocity u_* and Obukhov length L (in conjunction with the surface roughness length z_0). Light winds and extreme atmospheric stratification, associated with small magnitudes of u_* and L, limit the applicability of MO. Several studies show a deterioration in the accuracy of MO–LS emission calculations as u_* and $|L|$ decrease (e.g., Flesch et al., 2004; Gao et al., 2009), which has led to the introduction of filtering criteria to remove periods when u_* and $|L|$ fall below threshold values. For example, Flesch et al. (2005) used thresholds of $u_{*\mathrm{thres}} = 0.15\,m\,s^{-1}$ and $|L|_{\underline{\mathrm{thres}}} = 10\,m$, McBain

[1] The MO–LS designation can include backward Lagrangian stochastic (bLS) calculations for area sources, or a corresponding forward calculation (fLS) for point sources.

* Corresponding author. Tel.: +1 780 492 5406.
E-mail address: thomas.flesch@ualberta.ca (T.K. Flesch).

http://dx.doi.org/10.1016/j.agrformet.2014.07.010
0168-1923/

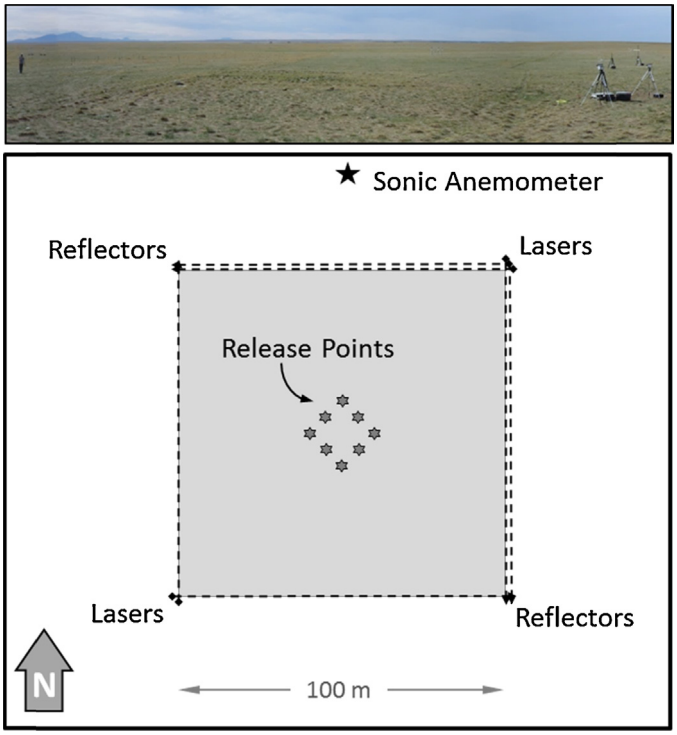

Fig. 1. Field site (top) and equipment and gas release configuration (bottom).

and Desjardins (2005) suggested $u_{*thres} = 0.19\ m\ s^{-1}$, while Laubach et al. (2008) used $0.12\ m\ s^{-1}$.

A consequence of filtering is the loss of potentially valuable data. With $u_{*thres} = 0.15\ m\ s^{-1}$ our experience has been of data loss rates of 40 to 50%, and sometimes more than 75% in long term rural studies (clearly this loss depends on the regional climate and the weather encountered during a campaign). The loss of low wind speed data hinders efforts to characterize sources having an emission rate that correlates with wind speed (e.g., ammonia from waste ponds), since emissions during light winds are unresolved. And because filtering preferentially removes light wind nighttime data, a daytime-biased dataset is created. This complicates the calculation of average emissions from diurnally varying sources, such as animals or industrial sites having a daily activity pattern.

The focus of this study is the filtering criteria used in MO–LS calculations. Our motivation comes from the perspective of animal studies, where the loss of nighttime data is a significant problem for characterizing emissions. We will examine the potential of u_*, L, wind speed and air temperature as filtering criteria, and consider how these affect MO–LS accuracy and the rate of data retention (particularly at night). A tracer release study, designed to mimic the configuration of a small herd of cattle, provides a large dataset for this evaluation.

2. Methods

2.1. Tracer release experiment

A tracer release experiment was conducted in September 2012 at Onefour, Alberta, Canada (49°06′N; 110°30′W; elevation 925 m). This semi-arid grassland site was selected because of its extensive short grass terrain and the absence of nearby gas sources (Fig. 1). The study was designed to mimic the configuration of a small herd of cattle. Eight release points were clustered near the centre of an imaginary 100×100 m square paddock (Fig. 1), at a height of 0.5 m above ground. Methane was released at a known rate using a mass flow controller (GFC47, AALBORG, Orangeburg, NY, USA) and verified by weighing of gas cylinders. The gas was directed to a manifold and distributed to the release points. The combination of a large diameter manifold and long and equal length tubing was assumed to give equal emission rates from each release point. The total release rate was either 0.46 or 0.92 kg CH_4 h^{-1} (equivalent to 50 to 150 cattle: a large release rate chosen to minimize concentration measurement errors). Releases took place intermittently from September 3 to 10, with a total of 215 15-min release periods. Of these, 144 occurred during the night (sunset to sunrise).

2.2. Concentration and wind measurements

Open-path CH_4 lasers (GasFinder 2, Boreal Laser Inc., Edmonton, Canada) measured the average gas concentration along the four sides of the simulated paddock. There were four stand-alone lasers and one laser on a pan-tilt head that scanned between two retro-reflectors (DSM; PTU D300, FLIR Motion Control Systems, Burlingame, CA, USA). This setup gave measurement duplication on two of the four paddock sides. The average path heights of the four laser lines varied from 1.5 to 2.15 m due to gentle terrain undulations.

Laser calibration was completed after the study. Recently, GasFinder lasers were found to have a previously unaccounted for temperature and pressure dependence (discussed by Laubach et al., 2013). This has been addressed by Boreal Laser Inc. in a new calibration procedure that gives temperature and pressure correction factors, and our lasers were re-calibrated after the study and these corrections were applied retroactively. Laser calibrations were also adjusted to match on-site measurements from a gas chromatograph (GC). Air samples were collected during a single 15-min interval between release periods, and laser-specific ratiometric correction factors were applied to force agreement between the lasers and the GC measured concentration (1.77 ppm_v).

Laser measurements were processed to give 15-min average concentrations. Concentrations were converted from the reported ppm_v to g m^{-3} using measured air pressure and temperature. Laser observations were not used if a 15-min period did not include more than 25% good data (i.e., light levels > 2000 units and R2 > 96: quality parameters reported by the laser).

A 3-D sonic anemometer (CSAT-3, Campbell Scientific, Logan, UT, USA) provided the wind information for our calculations: friction velocity u_*, Obukhov length L, surface roughness length z_0, and wind direction β (calculated as described in Flesch et al., 2004). The anemometer was positioned just north of the release site at a height of 2.0 m above ground. Wind statistics were calculated for 15-min intervals matching the CH_4 concentration record.

2.3. MO–LS emission calculations

Emission rates were calculated using the freely available WindTrax software. The software combines the MO–LS model described by Flesch et al. (2004) with mapping capabilities. Dispersion from each release point was simulated with a forward LS model using 10,000 trajectories. Identical emission rates were assigned to the eight release points in the calculation. From each set of 15-min laser concentrations, WindTrax calculated the total emission rate Q_{LS} (kg CH_4 h^{-1}) and the corresponding background concentration C_b. This problem is mathematically over-determined (e.g., six concentrations used to solve for two unknowns) and a best-fit procedure was used in the WindTrax calculation.

In the following analysis 19 out of the 214 release periods (15-min each) are not used. Fifteen had a calculated z_0 greater than the source height of 0.5 m; one period violated the Cauchy–Schwarz inequality (error in calculated wind statistics that can occur in light winds); in one extremely stable nighttime period the calculated

gas plumes did not reach the height of the laser paths; and in two periods a critical downwind laser observation was missing.

2.4. Temperature and wind speed profile

Air temperature (T) and wind speed (U) were measured with sonic anemometers (CSAT-3) at 1.0 and 2.9 m above ground. These instruments were in addition to our primary anemometer placed at a height of 2 m. Sonic anemometers measure acoustic temperature, which is related to the actual air temperature as (Kaimal and Gaynor, 1991):

$$T_{\text{son}} = T\left(1 + \frac{0.32e}{p}\right) \quad , \tag{1}$$

where e is the water vapor pressure and p is the absolute air pressure[2]. In this study our interest is the height gradient in T. Differentiating Eq. (1) gives:

$$\frac{\partial T_{\text{son}}}{\partial z} = \frac{\partial T}{\partial z}\left(1 + \frac{0.32e}{p}\right) + 0.32T\left(\frac{1}{p}\frac{\partial e}{\partial z} - \frac{e}{p^2}\frac{\partial p}{\partial z}\right) \quad . \tag{2}$$

For realistic values of p and e at our site (e.g., gradients consistent with latent heat fluxes <50 W m^{-2}) the difference between the height gradients of T_{son} and T is <0.05 K m^{-1}. This is much smaller than the magnitude of the temperature gradients we will be concerned with, and we thus assume a height difference ΔT_{son} equals the difference in actual temperature ΔT.

It is known that T_{son} can have an instrument specific bias due to uncertainties in the sonic path length. In their study of CSAT-3 anemometers, Burns et al. (2012) used an offset to correct for this. For moderate winds and neutral stratification we expect T_{son} to be nearly identical between our anemometers. In these conditions two anemometers were in very good agreement. The third was systematically cooler, and an offset of 0.25 K was applied.

3. Results

In the analysis that follows, each emission rate calculation Q_{LS} is expressed as a ratio of the actual emission rate Q, with $Q_{\text{LS}}/Q = 1$ being a perfectly accurate calculation. A good filtering procedure is judged to be one that results in a set of MO–LS observations having an average Q_{LS}/Q near 1 (good overall accuracy), a small standard deviation $\sigma_{Q/Q}$ (good period-to-period fidelity), and minimal data loss. We assume the tracer release rate, gas concentrations, wind statistics, and the location of lasers and sources are measured accurately, and that the MO–LS model describes turbulent dispersion during winds that are consistent with MO theory. This assumption of "no measurement error" is clearly false, but we believe these errors are small enough so that errors associated with an inaccurate MO description of the wind will be revealed over our large dataset.

For all 195 release periods (unfiltered) the average Q_{LS}/Q is 1.27 and $\sigma_{Q/Q} = 2.00$; meaning calculated emissions are 27% higher than the actual rate on average, and there is poor period-to-period fidelity. This is a poorer result than reported by Gao et al. (2009) for their unfiltered data ($Q_{\text{LS}}/Q = 1.04$, $\sigma_{Q/Q} = 0.55$), but almost identical to the unfiltered results reported by Flesch et al. (2004); $Q_{\text{LS}}/Q = 1.27$, $\sigma_{Q/Q} = 2.07$. Plotting Q_{LS}/Q with u_* and $1/L$ (Fig. 2) shows the expected trend toward less accurate inversions in light winds and stable conditions—typical nighttime conditions. Also notice that our dataset includes more stable than unstable periods, reflecting our interest in nighttime conditions, which limits our ability to assess filtering during unstable daytime conditions.

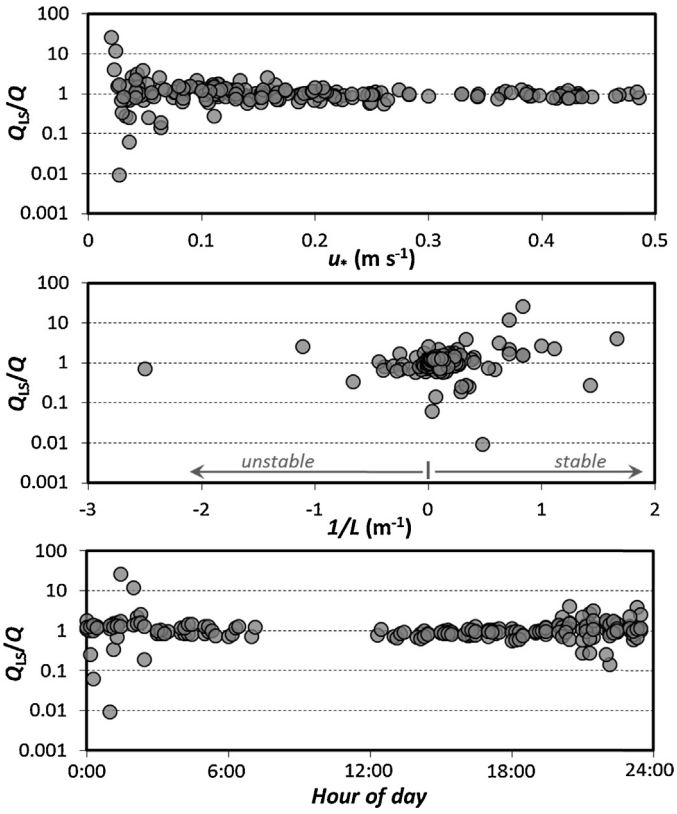

Fig. 2. Calculated emission rate (Q_{LS}/Q) plotted with friction velocity (u_*), the reciprocal of the Obukhov length ($1/L$), and hour of day (12:00 is local noon). A $Q_{\text{LS}}/Q = 1$ is perfect accuracy (notice the logarithmic scale).

3.1. Filtering with u_*

Flesch et al. (2004) reported that $u_* \leq 0.15$ m s^{-1} was the single best diagnostic for identifying inaccurate Q_{LS} in their tracer experiment. In the present context, using a $u_{*\text{thres}} = 0.15$ m s^{-1} filter leads to a substantial improvement in accuracy, with the average Q_{LS}/Q falling from 1.27 to 0.96, and $\sigma_{Q/Q}$ dropping from 2.00 to 0.19. This confirms what has been reported in many studies, that MO–LS is accurate in moderate to strong wind conditions. However, the cost of filtering is the loss of 50% of our data, and almost 75% of our nighttime data. Can $u_{*\text{thres}}$ be reduced from 0.15 m s^{-1} in order to increase data retention while still maintaining Q_{LS} accuracy?

Fig. 3 shows Q_{LS} accuracy for different u_* ranges. When $u_* < 0.05$ m s^{-1} the quality of Q_{LS} is very poor (average $Q_{\text{LS}}/Q = 2.69$, $\sigma_{Q/Q} = 5.15$) and most observations are in error by more than 50%. We conclude there is little potential for "recovering" accurate Q_{LS} at these low values of u_*. The situation improves for u_* between 0.05 and 0.15 m s^{-1} (average $Q_{\text{LS}}/Q = 1.14$, $\sigma_{Q/Q} = 0.47$). This is encouraging, as this u_* group accounts for nearly 40% of our data. Because the overall accuracy of this low u_* group is not particularly bad, one might simply include these data in an emission analysis. However, more than 20% of the observations in this group are outliers having $0.5 > Q_{\text{LS}}/Q > 1.5$. Outliers can be a problem with a small population of observations, e.g., a dataset divided in order to calculate hourly emission rates. Below we describe our attempts to discriminate the accurate and inaccurate Q_{LS} in this group having $0.05 \leq u_* < 0.15$ m s^{-1}.

[2] In applying Eq. (1) to average temperatures (via Reynolds's averaging) we assume the fluctuating term $e'T'$ is negligible, and that pressure fluctuations are a very small fraction of the average pressure and can be ignored.

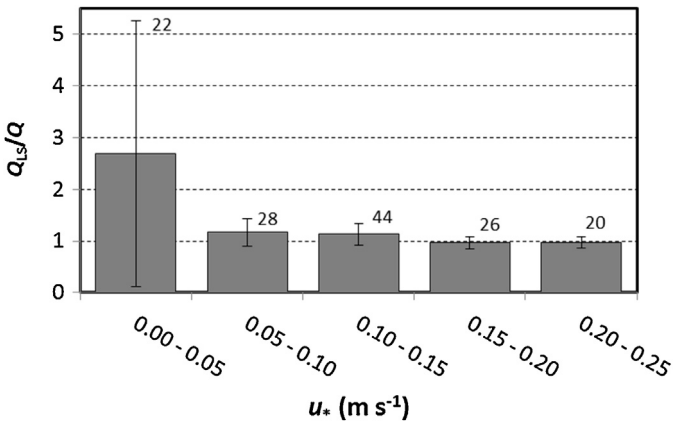

Fig. 3. Accuracy of the calculated emission rate (Q_{LS}/Q) grouped by friction velocity (u_*). The height of the "error bars" represents $\sigma_{Q/Q}$ for each group. Values above each column give the number of observations in the group.

3.2. Stability as a filtering criterion

Some studies have used atmospheric stability as a filtering criterion for MO–LS (Flesch et al., 2005; McGinn et al., 2011); rejecting observations having an Obukhov length L below a threshold $|L|_{\text{thres}}$. Lowering $|L|_{\text{thres}}$ results in the inclusion of periods with increasingly stable or unstable stratification. In Fig. 4 we see the result of imposing different $|L|_{\text{thres}}$ values on the target $0.05 \le u_* < 0.15$ m s^{-1} group. No substantial improvement in the accuracy of the inversion Q_{LS} is observed using a stability filter.

3.3. Temperature gradient as a filtering criterion

A comparison between the measured and MO predicted temperature gradient may indicate an inaccurate MO description of the atmosphere, and inaccurate MO–LS calculations. The difference in T between heights z_1 and z_2 is given by the MO formula[3] (Garratt, 1992):

$$\Delta T_{MO} = \frac{u_*^2 T_{\text{ave}}}{k_v^2 g L}\left[\ln\left(\frac{z_2}{z_1}\right) - \Psi_H(z_2) + \Psi_H(z_1)\right] \quad (3)$$

where T_{ave} is the average air temperature (K, here taken at $z = 2$ m), k_v is von Karman's constant (0.4), g is the gravitational acceleration (9.81 m s^{-2}), and Ψ_H is a stability correction function:

$$\begin{cases} \Psi_H = 2\ \ln[(1+\sqrt{1-16z/L})/2] & , \quad (\text{for}\ \ L<0) \\ \quad\ = -5z/L & , \quad (\text{for}\ \ L>0) \end{cases} \quad (4)$$

For each measurement period we calculate the difference between the measured and MO-calculated gradient ($\Delta T - \Delta T_{\text{MO}}$) evaluated at $z = 1$ and 2.9 m. Hereafter, we refer to ($\Delta T - \Delta T_{\text{MO}}$) as $\Delta\Delta T$. A filter is created to reject periods when $|\Delta\Delta T|$ is greater than a threshold $|\Delta\Delta T|_{\text{thres}}$.

Fig. 4 shows the impact of the $\Delta\Delta T$ filter on the target $0.05 \le u_* < 0.15$ m s^{-1} group. As $|\Delta\Delta T|_{\text{thres}}$ decreases from 2.0 to 0.25 K we see improvement in the average Q_{LS}/Q from 1.13 to 1.01, with a slight improvement in $\sigma_{Q/Q}$ from 0.24 to 0.18. The choice $|\Delta\Delta T|_{\text{thres}} = 0.5$ K eliminates the worst Q_{LS} outliers and retains 74% of this u_* group.

[3] This formula is for potential temperature. Over a small height difference it can be applied to actual temperature.

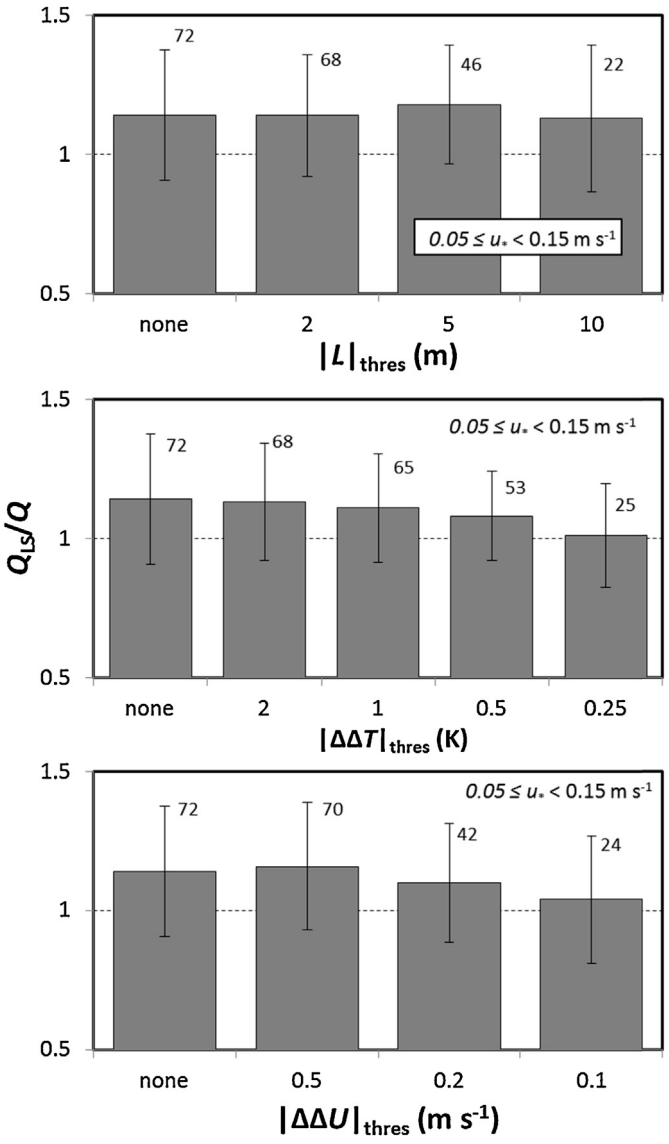

Fig. 4. Accuracy of the calculated emission rate (Q_{LS}/Q) as affected by filtering criteria based on the Obukhov length L, temperature errors $\Delta\Delta T$, and wind speed errors $\Delta\Delta U$. The height of the "error bars" represents $\sigma_{Q/Q}$ for each group, and the values above each column give the number of observations. These results are for periods having $0.05 \le u_* < 0.15$ m s^{-1}.

3.4. Wind speed as a filtering criterion

Along the same lines as the temperature gradient, a comparison between predicted and measured wind speed (U) may provide an alternative indication of MO failure. The difference in U between heights z_1 and z_2 is given by the MO formula (Garratt, 1992):

$$\Delta U_{MO} = \frac{u_*}{k_v}\left[\ln\left(\frac{z_2}{z_1}\right) - \Psi_M(z_2) + \Psi_M(z_1)\right] \quad (5)$$

where Ψ_M is a stability correction function. We use:

$$\begin{cases} \Psi_M(z) = 2\ \ln[(1+x)/2] + \ln[(1+x^2)/2] - 2\tan^{-1}x + \pi/2], & (\text{for}\ L<0) \\ \quad\ = -5\,z/L & , \quad (\text{for}\ \ L>0) \end{cases} \quad (6)$$

where $x = (1-16z/L)^{1/4}$. With Eq. (5) we compare the difference between measured and calculated ΔU for $z = 1$ and 2.9 m ($\Delta U - \Delta U_{\text{MO}}$), hereafter referred to as $\Delta\Delta U$. A filter is used to reject periods when $|\Delta\Delta U|$ is greater than a threshold $|\Delta\Delta U|_{\text{thres}}$.

Fig. 4 shows the impact of the $\Delta\Delta U$ filter on the $0.05 \le u_* < 0.15$ m s^{-1} group. There is modest improvement in

Table 1
Effect of filtering strategies on MO–LS results.

	No filter	Filtering options			
		$u_{*\text{thres}} = 0.15\ \text{m s}^{-1}$	$u_{*\text{thres}} = 0.05\ \text{m s}^{-1}$	$\lvert\Delta\Delta T\rvert_{\text{thres}} = 0.5$ K	$u_{*\text{thres}} = 0.05\ \text{m s}^{-1}$, $\lvert\Delta\Delta T\rvert_{\text{thres}} = 0.5$ K
Average Q_{LS}/Q ($\sigma_{Q/Q}$)					
Total	1.27 (2.00)	0.96 (0.19)	1.04 (0.35)	1.02 (0.30)	1.00 (0.25)
Daytime	0.90 (0.16)	0.89 (0.14)	0.90 (0.16)	0.90 (0.16)	0.90 (0.16)
Nighttime	1.47 (2.47)	1.09 (0.18)	1.14 (0.41)	1.13 (0.35)	1.09 (0.28)
Observations					
Total	195	96	168	153	149
Daytime	70	63	70	70	70
Nighttime	125	33	98	83	79
Data Retention					
Total	100%	49%	86%	78%	76%
Daytime	100%	90%	100%	100%	100%
Nighttime	100%	26%	78%	66%	63%

the average accuracy of Q_{LS}/Q as the threshold declines from 0.5 to 0.1 m s^{-1}. There is no improvement in $\sigma_{Q/Q}$ however, and the data loss with the $\Delta\Delta U$ filter is greater than with the $\Delta\Delta T$ filter for a similar improvement in Q_{LS} accuracy. We conclude that $\Delta\Delta U$ is not as successful as a criterion based on $\Delta\Delta T$.

4. Discussion

Our study corroborates earlier work showing good accuracy in Q_{LS} during higher wind speeds ($u_* \geq 0.15\ \text{m s}^{-1}$). However, in many experiments a significant portion of observations occur at low wind speeds, and increasing data retention requires identifying low wind periods when accurate inversions are likely to occur. At the lowest wind speeds, when $u_* < 0.05\ \text{m s}^{-1}$, the possibility of an accurate calculation appears low. But with $0.05 \leq u_* < 0.15\ \text{m s}^{-1}$, we found observations having a mix of accurate and inaccurate inversions. A measurement of $\Delta\Delta T$ helped to discriminate those two outcomes.

We now consider four filtering strategies applied to our full dataset (including high wind speed periods). The first uses only the stringent $u_{*\text{thres}} = 0.15\ \text{m s}^{-1}$ filter, used in previous MO–LS studies. The second relaxes this to $u_{*\text{thres}} = 0.05\ \text{m s}^{-1}$. The filter $\lvert\Delta\Delta T\rvert_{\text{thres}} = 0.5$ K acts alone in our third strategy. And finally, we combine $u_{*\text{thres}} = 0.05\ \text{m s}^{-1}$ and $\lvert\Delta\Delta T\rvert_{\text{thres}} = 0.5$ K. The impact of these filters is summarized in Table 1. Several things to note:

- Filtering has little effect on daytime results. Even the most restrictive filter ($u_{*\text{thres}} = 0.15\ \text{m s}^{-1}$) results in a small daytime data loss. While we see no benefit in daytime filtering in our dataset, with only seven periods having very unstable stratification ($|L| < 5$ m) we are limited in assessing filtering in unstable daytime conditions.
- Filtering has a large impact at night. Each filter improves the average Q_{LS}/Q over the unfiltered data, although the difference in average accuracy between the four filters is small. The greater difference is in the data rejection rate and $\sigma_{Q/Q}$. The combination $u_{*\text{thres}} = 0.05\ \text{m s}^{-1}$ and $\lvert\Delta\Delta T\rvert_{\text{thres}} = 0.5$ K is a good compromise of accuracy, period-to-period precision, and high data retention.
- Q_{LS}/Q is negatively biased during the day, and positively biased at night (statistically different from 1.0 in all cases: t-test with $P = 0.9$). This is consistent with earlier MO–LS observations of a negative/positive bias in unstable/stable stratification (Flesch et al., 2004; Gao et al., 2009). We note the possibility that this bias is an artifact of laser temperature sensitivity. The Q_{LS}/Q is correlated with T ($r = -0.41$), and this is consistent with a greater sensitivity to T than indicated by the factory calibration[4].

[4] Laubach et al. (2013) found greater T sensitivity in their Boreal laser than reported in our factory calibrations.

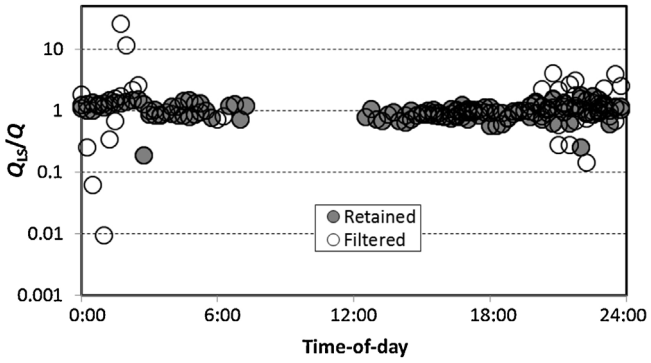

Fig. 5. The Q_{LS}/Q plotted with time-of-day (12:00 = local noon). The open circles are data that would be removed by filtering with $u_{*\text{thres}} = 0.05$ m s^{-1} and $\lvert\Delta\Delta T\rvert_{\text{thres}} = 0.5$ K.

Fig. 5 shows the effect of the ($u_{*\text{thres}} = 0.05\ \text{m s}^{-1}$, $\lvert\Delta\Delta T\rvert_{\text{thres}} = 0.5$ K) filter on our full dataset. This filter combination eliminates most of the Q_{LS} outliers while retaining 76% of the data. In particular, this filter more than doubles the nighttime data retention of the $u_{*\text{thres}} = 0.15\ \text{m s}^{-1}$ filter.

From Table 1 we could conclude that adding $\Delta\Delta T$ as a filtering criterion, in addition to a relaxed $u_{*\text{thres}} = 0.05\ \text{m s}^{-1}$ criterion, results in only a minor improvement in MO–LS accuracy (e.g., the nighttime average Q_{LS}/Q improved slightly from 1.14 to 1.09). However, this may understate the potential benefit of $\Delta\Delta T$ in discriminating Q_{LS} outliers. In animal studies for example, hourly emission rates may be needed to establish a diurnal emission relationship (e.g. McGinn et al., 2011). Even a large dataset may have a small number of data points in a given hourly interval, and the presence of an outlier can have a large impact. For example, over the 02:00–03:00 interval of our dataset, the $\Delta\Delta T$ filter reduces Q_{LS}/Q from 1.38 to 1.06 compared with the single $u_{*\text{thres}} = 0.05\ \text{m s}^{-1}$ criterion. Another benefit with the $\Delta\Delta T$ filter is a reduction in the random period-to-period error as reflected in $\sigma_{Q/Q}$. Adding the supplementary $\Delta\Delta T$ filter reduces $\sigma_{Q/Q}$ by approximately 30%. Statistically, this reduction increases the ability to detect emission differences between populations or treatments.

5. Conclusions

A filtering strategy with $u_{*\text{thres}} = 0.05\ \text{m s}^{-1}$ and $\lvert\Delta\Delta T\rvert_{\text{thres}} = 0.5$ K gave a good combination of Q_{LS} accuracy and high data retention rates. The value of adding $\Delta\Delta T$ as part of a refined filtering strategy ultimately depends on the importance of accurate nighttime data. For some types of emission sources the retention of nighttime data is unimportant. For example, CH_4 produced from

decomposition in deep ponds may have neither a diurnal trend nor wind speed correlation (i.e., emissions are a function of a slowly varying deep bottom temperature). In this case daytime measurements may adequately establish the average emission rate, and applying a larger $u_{*\mathrm{thres}}$ filter to liberally eliminate potential errors is a wise choice. But if emissions vary diurnally (e.g., animals) or correlate with wind speed (e.g., ammonia from soils), retaining light wind nighttime data is important.

The use of this $|\Delta\Delta T|_{\mathrm{thres}} = 0.5$ K criterion is specific to our measurement heights of 1 and 3 m (nominally). Ideally we would prefer a non-dimensional measure of temperature error, such as the fractional error $\Delta T/\Delta T_{\mathrm{MO}}$. However, as ΔT_{MO} is often near zero, large fractional errors occur even when the absolute accuracy is good. Alternatively, one might express the ΔT error in gradient form as $|(\Delta T/\Delta z)–(\Delta T/\Delta z)_{\mathrm{MO}}|$ to increase generality across a range of measurement heights. However, the non-linearity of the temperature profile near ground means this will also be a height dependent criterion.

Acknowledgements

Funding provided by the CSIRO Sustainable Agriculture Flagship, the Canadian Agricultural Greenhouse Gases Program, and Agriculture and Agri-Food Canada's Growing Forward Program. The technical support of Trevor Coates is gratefully acknowledged. The helpful comments of two anonymous reviewers were appreciated.

References

Burns, S.P., Horst, T.W., Jacobsen, L., Blanken, P.D., Monson, R.K., 2012. Using sonic anemometer temperature to measure sensible heat flux in strong winds. Atmos. Meas. Tech. 5, 2095–2111.

Ferrara, R.M., Loubet, B., Decuq, C., Palumbo, A.D., Di Tommasi, P., Magliulo, V., Masson, S., Personne, E., Cellier, P., Rana, G., 2014. Ammonia volatilisation following urea fertilisation in an irrigated sorghum crop in Italy. Agric. For. Meteorol. 195–196, 179–191.

Flesch, T.K., Verge, X.P.C., Desjardins, R.L., Worth, D., 2013. Methane emissions from a swine manure tank in western Canada. Can. J. Anim. Sci. 93, 159–169.

Flesch, T.K., Wilson, J.D., Harper, L.A., Crenna, B.P., 2005. Estimating gas emission from a farm using an inverse-dispersion technique. Atmos. Environ. 39, 4863–4874.

Flesch, T.K., Wilson, J.D., Harper, L.A., Crenna, B.P., Sharpe, R.R., 2004. Deducing ground-air emissions from observed trace gas concentrations: a field trial. J. Appl. Meteorol. 43, 487–502.

Gao, Z., Mauder, M., Desjardins, R.L., Flesch, T.K., van Haarlem, R.P., 2009. Assessment of the backward Lagrangian Stochastic dispersion technique for continuous measurements of CH_4 emissions. Agric. For. Meteorol. 149, 1516–1523.

Garratt, J.R., 1992. The Atmospheric Boundary Layer. Cambridge University Press, New York, NY, pp. 316.

Harper, L.A., Flesch, T.K., Wilson, J.D., 2010. Ammonia emissions from broiler production in the San Joaquin Valley. Poult. Sci. 89, 1802–1814.

Kaimal, J.C., Gaynor, J.E., 1991. Another look at sonic thermometry. Bound. Layer Meteorol. 56, 401–410.

Laubach, J., Kelliher, F.M., Knight, T.W., Clark, H., Molano, G., Cavanagh, A., 2008. Methane emissions from beef cattle: a comparison of paddock and animal-scale measurements. Aust. J. Exp. Agric. 48, 132–137.

Laubach, J., Bai, M., Pinares-Patino, C.S., Phillips, F.A., Naylor, T.A., Molano, G., Rocha, E.A.C., Griffith, D.W.T., 2013. Accuracy of micrometeorological techniques for detecting a change in methane emissions from a herd of cattle. Agric. For. Meteorol. 176, 50–63.

McBain, M.C., Desjardins, R.L., 2005. The evaluation of a backward Lagrangian stochastic (BLS) model to estimate greenhouse gas emissions from agricultural sources using a synthetic tracer source. Agric. For. Meteorol. 135, 61–72.

McGinn, S.M., Turner, D., Tomkins, N., Charmley, E., Bishop-Hurley, G., Chen, D., 2011. Methane emissions from grazing cattle using point-source dispersion. J. Environ. Qual. 40, 22–27.

Sanz, A., Misselbrook, T., Sanz, M.J., Vallejo, A., 2010. Use of an inverse dispersion technique for estimating ammonia emission from surface-applied slurry in Central Spain. Atmos. Environ. 44, 999–1002.

Todd, R.W., Cole, N.A., Rhoades, M.B., Parker, D.B., Casey, K.D., 2011. Daily, monthly, seasonal and annual ammonia emissions from southern high plains cattle feedyards. J. Environ. Qual. 40, 1–6.

Wilson, J.D., Flesch, T.K., Crenna, B.P., 2012. Estimating surface-air gas fluxes by inverse dispersion using a backward Lagrangian stochastic trajectory model. In: Lin, J., Brunner, D., Gerbig, C., Stohl, A., Luhar, A., Webley, P. (Eds.), Lagrangian Models of the Atmosphere. AGU Geophysical Monograph 200. American Geophysical Union, Washington D.C, pp. 149–161.